MAX-PLANCK-INSTITUT FÜR PLASMAPHYSIK

GARCHING BEI MÜNCHEN

Absorption and Scattering of Neutral Particle Beams used for the Determination of Plasma Parameters

H.M. Mayer

IPP IV/80 February 1975

Die nachstehende Arbeit wurde im Rahmen des Vertrages zwischen dem Max-Planck-Institut für Plasmaphysik und der Europäischen Atomgemeinschaft über die Zusammenarbeit auf dem Gebiete der Plasmaphysik durchgeführt.

IPP IV/80

H.M. Mayer

Absorption and Scattering of Neutral Particle Beams used for the Determination of Plasma Parameters

February 1975 (in English)

Abstract

The processes which dominate the passage of neutral particle beams through a fully ionized hydrogen plasma are analyzed from a diagnostic point of view. In particular He and Ne beams are considered as they are the most penetrating ones which can give pronounced limiting angle scattering.
The dependence of attenuation on T_e, T_i of a He beam and the scattering of a Ne beam are discussed in more detail.

Introduction

As almost every plasma parameter can affect the passage of a neutral particle beam, it should be possible to evalue almost any plasma quantity from the passage of such beams. Limitation, however, arises from the following facts:

1) the penetration depth is limited by ionization and charge exchange.

2) the functional dependence on plasma parameters is generally complex and may be not very pronounced.

3) In general the cross-section for Coulomb interaction of a beam particle of nuclear charge $Z_B e$ with a target ion of charge $Z_T e$ is proportional to $(Z_B Z_T e^2)^2$ which attributes a very important role to the presence of high Z impurities. (In some situations, a virtue can be made out of the necessity and a tool for impurity diagnostics is obtained).

4) Often the interpretation of the observed attenuation, angular distribution, energy spectra etc. in terms of plasma parameters suffers from a lack of accurate knowledge of the cross-sections involved.

Generally plasma diagnostics by neutral particle beams is still in a very early stage of its development and it is to be expected that applications will show up in the near future which are not foreseen at the moment.

Ionization by Electron Impact

For the beam particles we can define an effective attenuation cross-section by

$$\sigma_{AE} = \frac{\langle \sigma_{EI} v \rangle}{v_B} \qquad (1)$$

σ_{EI} = cross-section for ionization by electron impact

v = relative velocity $\approx v_{the}$

v_B = beam velocity

Ionization from the ground state is usually considered to be the dominant process. However, the cross-sections σ_ν^* for excitation into state ν are often comparable in order of magnitude and the effective cross-section for two-step processes will be of the order $\sum_\nu \sigma_\nu^*$ as soon as the mean free paths $\lambda_{i\nu}$ for ionization from states ν stay below the length of plasma traversed by the beam. It seems unlikely that the inclusion of stepwise ionization will change the total rate by much more than a factor 2 in most situations but one should be aware of this uncertainty whenever several mean free paths of plasma have to be traversed.

We have observed that the cross-sections for ionization from ground state can be approximated by

$$\frac{\sigma}{\sigma_M} = \frac{E_M}{E} e^{1 - E_M/E} \qquad (2)$$

where $\sigma_M(E_M)$ is the maximum value. This approximation describes rather well the experimental curves /1/ for H, H_2, He, Ne in the range of electron energies to be considered. With this approximation the integration over a Maxwellian distribution can be carried out analytically /2/ yielding

$$\langle \sigma v \rangle = \sigma_M v_M \frac{e}{\sqrt{\pi}} x^2 K_1(x) \; ; \; x = \left(\frac{4 E_M}{T_e}\right)^{1/2}$$

with $x^2 K_1(x) \xrightarrow{|x|<<1} x$ $\qquad v_M = \left(\frac{2 E_M}{m_e}\right)^{1/2}$ (3)

$$\mathrm{Max}\left[\frac{e}{\sqrt{\pi}} x^2 K_1(x)\right] \approx 1 \quad \text{at} \quad x_m = 1.32$$

In the log-log plot of Fig. 1 the curves obtained from Eq. (3) are parallel to each other. For the elements Ar, Kr, Xe /1/ only the position of the maximum is indicated. In these cases the approximation by Eq. (2) is not quite as good but may still yield a reasonable estimate.

Charge Exchange and Ionization by Ion Impact

For energies ϵ < 10 keV/nucleon charge exchange is dominant, whereas proton ionization prevails for ϵ > 100 keV/nucleon. In Fig. 2 both cross-sections have been added to a single curve. The references used are, CE: H^o/2,3,4/, He/5,6/ Ne/6/ PI: H^o/7,8/, He/6,9/, Ne/9,10/. The possibility of excitation and subsequent ionization also exists for proton impact but for non hydrogenic beams the beam velocity will usually be in a range where charge exchange is more important.

The ionization due to impact by multiply charged impurity ions is difficult to assess. If a Z^2-dependence of the cross-section is assumed and if the beam energy stays well below

the maximum for proton impact, it can be hoped that in moderately contaminated hydrogen plasmas ($Z_{eff} \lesssim 3$) this process does not change the absorption substantially.

Dependence of Absorption on ϵ

The $\epsilon^{-1/2}$ decrease of electronic absorption and the steep rise of ionic absorption combine to curves with a dip or a rather flat plateau in the intermediate region. This dip is most pronounced for large T_e and low T_i as shown in Fig. 3. The curves of this figure are only half-quantitative in nature. They are based on the rates for ionization of hydrogen by proton impact given in /11/ and use has been made of the fact that $(\sigma_{CE} + \sigma_{PI})_{He} \approx 2(\sigma_{PI})_{H^0}$ in the region of interest.

Disregarding effects which may arise from the presence of high Z impurities Fig. 3 demonstrates that once T_e, n_e are known this dependence could be used for a rough determination of an average $\langle T_i \rangle$ taken along the trajectory. For comparison another beam could be used which traverses the same length and the ϵ of which is chosen in the region of intersection. Calibration of the probing beam (chosen at lower energies) against this reference beam could then be made at low values of T_e where the absorption depends little on T_i and beam energy.

Depending on the dimensions of the plasma region to be probed as well as the ranges of T_i and T_e it may be possible to find beams of atoms (or molecules) which are more suited for this kind of $\langle T_i \rangle$ determination than He.

Scattering

In the following only multiple scattering and elastic single scattering is considered whereas inelastic scattering is ignored.

Abramov et al. /13/ have shown that - under rather general assumptions - elastic scattering by an angle ϑ in the laboratory leads to a Gaussian energy distribution of half-width ΔE given by

$$\Delta E = 4\vartheta [E T A \ln 2]^{1/2}, \quad \vartheta \ll 1 \tag{4}$$

where T is the temperature of target particles $A = M_B / M$ and where the beam velocity is assumed to be large compared to the thermal velocity.

For an atomic mass ratio $A > 1$ a maximum angle ϑ_M given by

$$\sin \vartheta_M = 1/A \tag{5}$$

exists beyond which beam particles cannot be scattered if the target particles are initially at rest. Thermal motion will dissolve this sharp limit into a Gaussian distribution of width

$$\langle (\vartheta - \vartheta_M)^2 \rangle = T/AE, \quad (\vartheta - \vartheta_M) \ll \vartheta \ll 1 \tag{6}$$

which is multiplied by a factor ϑ_M / ϑ to account for "radial diffusion". While Eq. (6) is based on a simplified argument a rigorous calculation for He has been made by Afrosimov and Kislyakov /14/ who proposed limiting angle scattering as a diagnostic tool.

We investigate in more detail the single scattering and multiple scattering regions.

Single Scattering.

When viewed from the laboratory $(\vartheta, d\omega)$ the Rutherford cross-section in the CM system $(\Theta, d\Omega)$ becomes

$$\frac{d\sigma_{SS}}{d\omega} = \left(\frac{e^2 Z_B Z_T}{\mu v^2}\right)^2 \frac{d\Omega/d\omega}{4\sin^4\Theta/2} \qquad \vec{v} = \vec{v}_B - \vec{v}_T \qquad \mu = \frac{M_B M_T}{M_B + M_T} = \frac{A_B \cdot M_H}{1+A}$$

$$= \frac{d\sigma_0}{d\omega} \cdot \frac{[1 + 1/A^2 + 2x/A]^{3/2}}{(1-x)^2(x+1/A)} \cdot A^2(A^2+1)^{-3/2} \xrightarrow{x=0} \frac{d\sigma_0}{d\omega} \tag{7}$$

$$\frac{d\sigma_0}{d\omega} = \left(\frac{1+A}{2}\right)^2 (1+A^2)^{3/2} Z_B^2 Z_T^2 r_e^2 \left(\frac{m_e c^2}{\varepsilon A_B}\right)^2$$

with

$A_B = M_B/M_H$, $A = M_B/M_T$, $x = \cos\Theta$, $r_e^2 = (e^2/m_e c^2)^2 = 8 \cdot 10^{-26}\,cm^2$

In Eq. (7) x is related to ϑ by

$$\sin\vartheta = \frac{(1-x^2)^{1/2}}{[1+1/A^2+2x/A]^{1/2}} \cdot \frac{1}{A} \tag{8}$$

Combining (7) and (8) yields the angular distribution in the laboratory. By separation of $d\sigma_0/d\omega$ we have normalized the cross-section to right-angle scattering in the CM-system leading to an angle ϑ_0 in the L-system given by

$$tg\,\vartheta_0 = \frac{1}{A} \quad \text{with} \quad \vartheta_M - \vartheta_0 \xrightarrow{A \gg 1} 1/2A^3 \tag{9}$$

This procedure is reasonable as the singularity at x = - 1/A is of the type $(\vartheta_M - \vartheta)^{-1/2}$ and will easily be washed out my multiple scattering (see below).

Multiple Scattering.

This process leads to a distribution of scattered beam intensity close to the beam axis given by

$$\frac{dI_{MS}}{d\vartheta} = \frac{2\vartheta\, e^{-\vartheta^2/\langle\vartheta^2\rangle_{MS}}}{\langle\vartheta^2\rangle_{MS}} I_0 \tag{10}$$

with

$$\langle\vartheta^2\rangle_{MS} \simeq \pi \left(4 Z_T \frac{Z_B}{A_B} r_e \frac{m_e c^2}{\varepsilon}\right)^2 \cdot N t_{MS}$$

where Nt_{MS} is the number of particles/cm^2 traversed.

From Eq. (10) it can be seen that multiple scattering can be used to determine the mean value $\langle Z_T^2\rangle$ along the beam trajectory

once the density profile is known.

For comparison with (7) we define an effective cross-section

$$\frac{d\sigma_{MS}}{d\omega} = \frac{dI_{MS}}{d\vartheta} / 2\pi N t_{ss} \sin\vartheta \, I_0 \qquad (11)$$

where t_{ss} is the depth of the scattering volume which is viewed from the detector. Curves calculated from Eqs. (7), (11) and (10) are shown in Fig. 4. Multiple scattering tends to wash out the limiting angle in the same way as does target particle temperature. However, instead of $\langle \vartheta^2 \rangle_{MS}$ from Eq. (10), we should now use the value $\langle \vartheta^2 \rangle = \langle \vartheta^2 \rangle_{MS} / 2^2$ for angles projected into the plane of scattering. From Eq. (6) the minimum detectable temperature due to multiple scattering will then be about

$$T_{min} \approx AE \langle \vartheta^2 \rangle_{MS} / 2 \quad \propto A/E \qquad (12)$$

Impurities.

For a heavy impurity ion (Z^*, M^*) with $A^* = M_B / M^* \ll 1$, we find from Eq. (7) a background of single scattering at ϑ_M of the magnitude

$$\frac{d\sigma^*}{d\sigma_0} \approx \frac{2 Z^{*2}}{(A^*+1)A} \qquad (13)$$

whereas for light impurities with $1 \ll A^* < A$ we have approximately

$$\frac{d\sigma^*}{d\sigma_0} \approx \frac{(A^*+1)^2}{A^{*3}} \frac{4A^4}{(A+1)^2 (A^2+1)^{3/2}} \approx \frac{4 Z^{*2}}{A^* A} \qquad (14)$$

Comparison between He and Ne beams.

From Eq. (12) the sensitivity of a Ne beam is 5 times lower than for a He-beam of same energy. Moreover from Fig. 2 it has considerably smaller penetration capacity. Nevertheless there are properties also which favour the Ne beam. From Eq. (7) the scattered intensity is higher by a factor $\approx 5^5$. In

addition the small value of $\vartheta_M = 3^o$ would allow to collect the entire azimuth with a conical arrangement.

Despite of this increase in total intensity the contribution from impurities will be about five times smaller for Ne than for He as may be seen from Eqs. (13) and (14). This is true if the Rutherford angular dependence $\propto \sin^{-4}(\Theta/2)$ still holds. Making use of the classical relation between impact parameter b and CM-angle Θ /15/

$$b = \frac{Z_B Z_T e^2}{\mu v^2 \operatorname{tg}(\Theta/2)} \tag{15}$$

and supposing very heavy ions for which $\mu \approx M_B$, $\Theta \approx \vartheta$, we find for ϑ chosen at $\vartheta_M = 1/A \ll 1$ and $Z_B = A_B/2$

$$b_M = \frac{A Z^*}{2} r_e \cdot \frac{m_e c^2}{\mathcal{E}} \tag{15}$$

If b_M becomes larger than the atomic radius $a \approx 1{,}4\, Z_B^{-1/3} a_o \approx (A_B)^{-1/3} a_o$ (where a_o is the Bohr radius) the beam atom becomes partly screened by its electronic shell. Equating a to b_M from Eq. (15) shows that this is the case for

$$Z^* \gtrsim 4{,}4 \cdot 10^4 \; A_B^{-1/3} A^{-1} \; \frac{\mathcal{E}}{m_e c^2} \tag{16}$$

For $\epsilon/m_e c^2 \approx 1/50$ screening should set in at $Z^* \approx 16$. Therefore the impurity contributions from Mo^{XX} and Mo^{XXX} as shown in Fig. 4 in fact may be exaggerated.

If collisions with $b_M \approx a$ would have a large probability for ionization or exitation into a state which is more likely to be ionized, this would of course be another very fortunate chance to get rid of high Z impurity background.

Finally, energy discrimination of the charge exchanged beam could be helpful to reject undesired background. Beam particles which are scattered at small angles from targets which are several times heavier suffer almost no energy loss whereas the loss from cold protons is $\Delta E_o = E/A$ around which the distribution for hot protons according to Eq. (4) is centered. The fact that the charge exchanged Ne beam has a greater magnetic stiffness than the charge exchanged He beam should facilitate discrimination from low mass number background.

Conclusions

Thedependence of neutral beam absorption on plasma parameters has been demonstrated. For electronic ionization from ground state an approximate analytical expression has been derived which is useful for simple atomic configurations. The dependence of beam absorption on proton temperature is demonstrated in the case of a He beam.

An example for the profile of a Ne-beam is shown of which the multiple scattering as well as the scattering beyond the limiting angle could be used in diagnostics. It is shown that for limiting angle scattering a Ne beam offers some attractive possibilities of intensity collection and background rejection which deserve to be weighed against its lower temperature sensitivity and penetration capacity when comparison with a He beam is made.

Acknowledgements

I want to thank Ch. Wharton for guidance into a new field; N.R. Heckenberg, K. McCormick, E. Speth and K.H. Steuer for discussions, Mrs. H. Pieper for help in preparing the manuscript.

References

/ 1/ Kieffer, L.J. et al. Rev. Mod. Phys. 38, 1 (1966)

/ 2/ Tables of Integral Transforms, Bateman Manuscript Vol I p. 146, McGrow-Hill (1954)

/ 3/ Belyaev, V.A. et al. Sov. Phys. JETP 25, 777 (1967)

/ 4/ Fite, W.L. et al. Phys. Rev. 112, 1161 (1958)

/ 5/ McClure, G.W. Phys. Rev. 148, 47 (1966)

/ 6/ Stedeford, J.B. H. and Hasted, J.B. Proc. R. Soc. A 227, 466 (1955)

/ 7/ Becher, M. and Scharmann A. Z. Naturf. 24, 854 (1969)

/ 8/ Fite, W.L. et al. Phys. Rev. 119, 663 (1960)

/ 9/ Gilbody, H.B. et al. Proc. Roy Soc. 227A, 137 (1964)

/10/ For further reference see McDaniel, E.W. Collision Phenomena in Ionized Gases (J. Wiley and Sons, New York 1964)

/11/ De Heer at al. Physica 32, 1766 (1966)

/12/ Rehker, S. and Speth, E. Max-Planck-Institut für Plasmaphysik, Report IPP 2/217 (1974)

/13/ Abramov V.G. et al. Sov. Phys. Techn. Phys. 16, 1520 (1972)

/14/ Afrosimov, V.V. and Kislyakov, A.I. Sov. Phys. Tech. Phys. 16, 1526 (1972)

/15/ See for instance ref. /10/ p. 431

Figures

Fig. 1 Rates for ionization from ground state as given by Eq. (3) in text

Fig. 2 Attenuation cross-sections for H^{o}-, He- and Ne beams

Fig. 3 Variation of the attenuation of a He beam with beam energy for various proton temperatures

Fig. 4 Scattering profile of a 200 keV Ne-beam

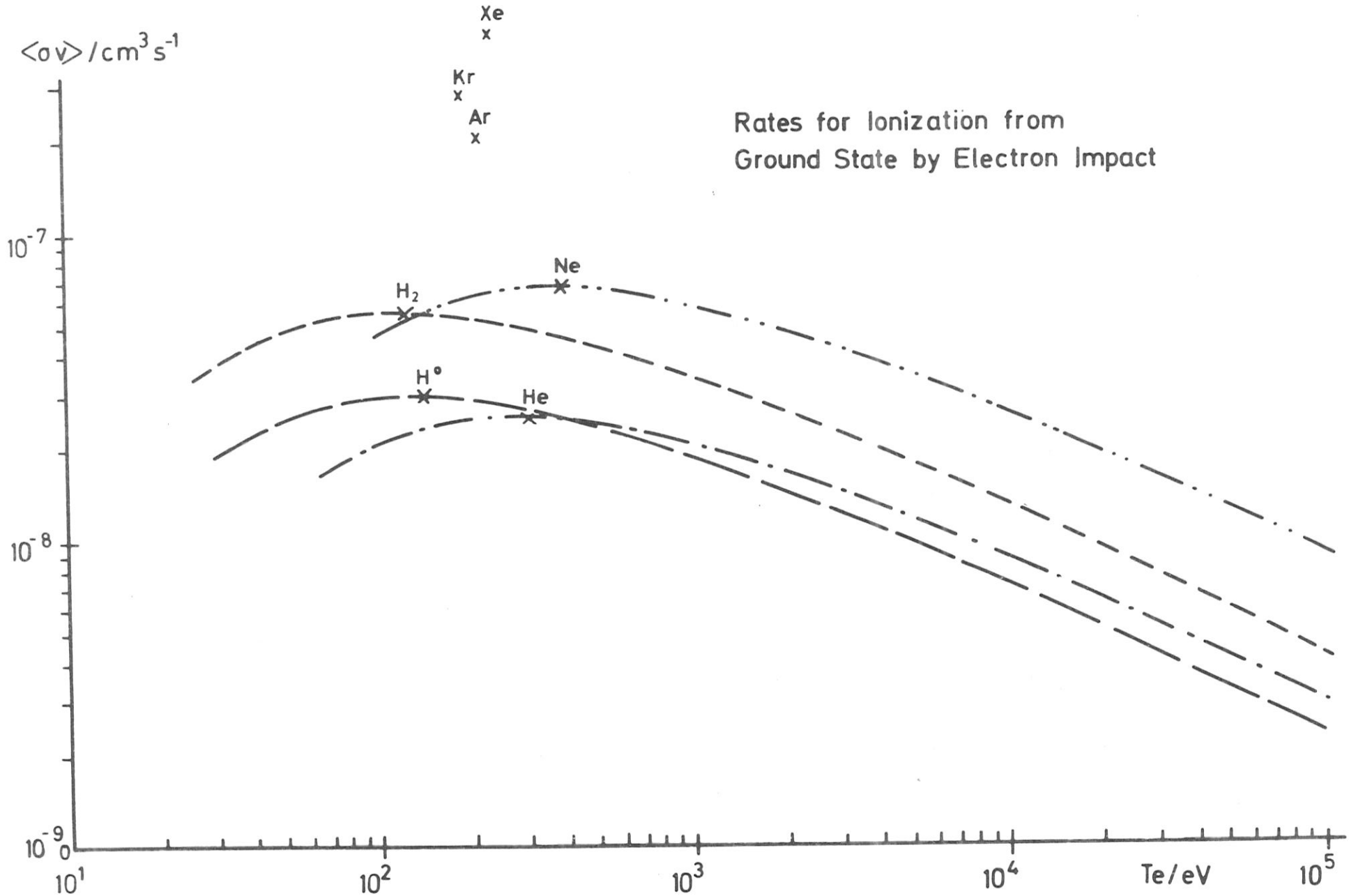

Fig. 1 Rates for ionization from ground state as given by Eq. (3) in text

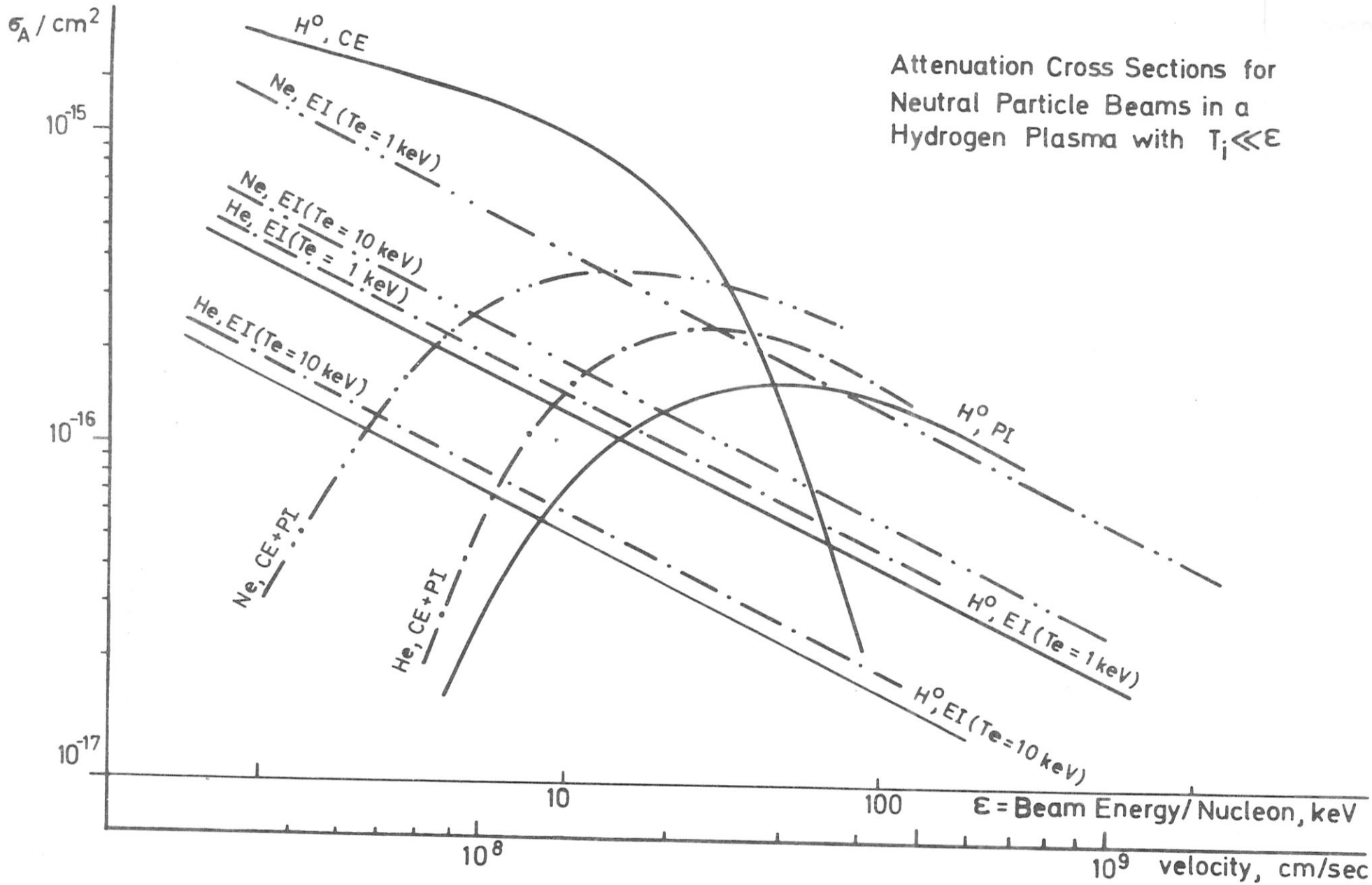

Fig. 2 Attenuation cross-sections for H^o-, Ne- and Ne beams

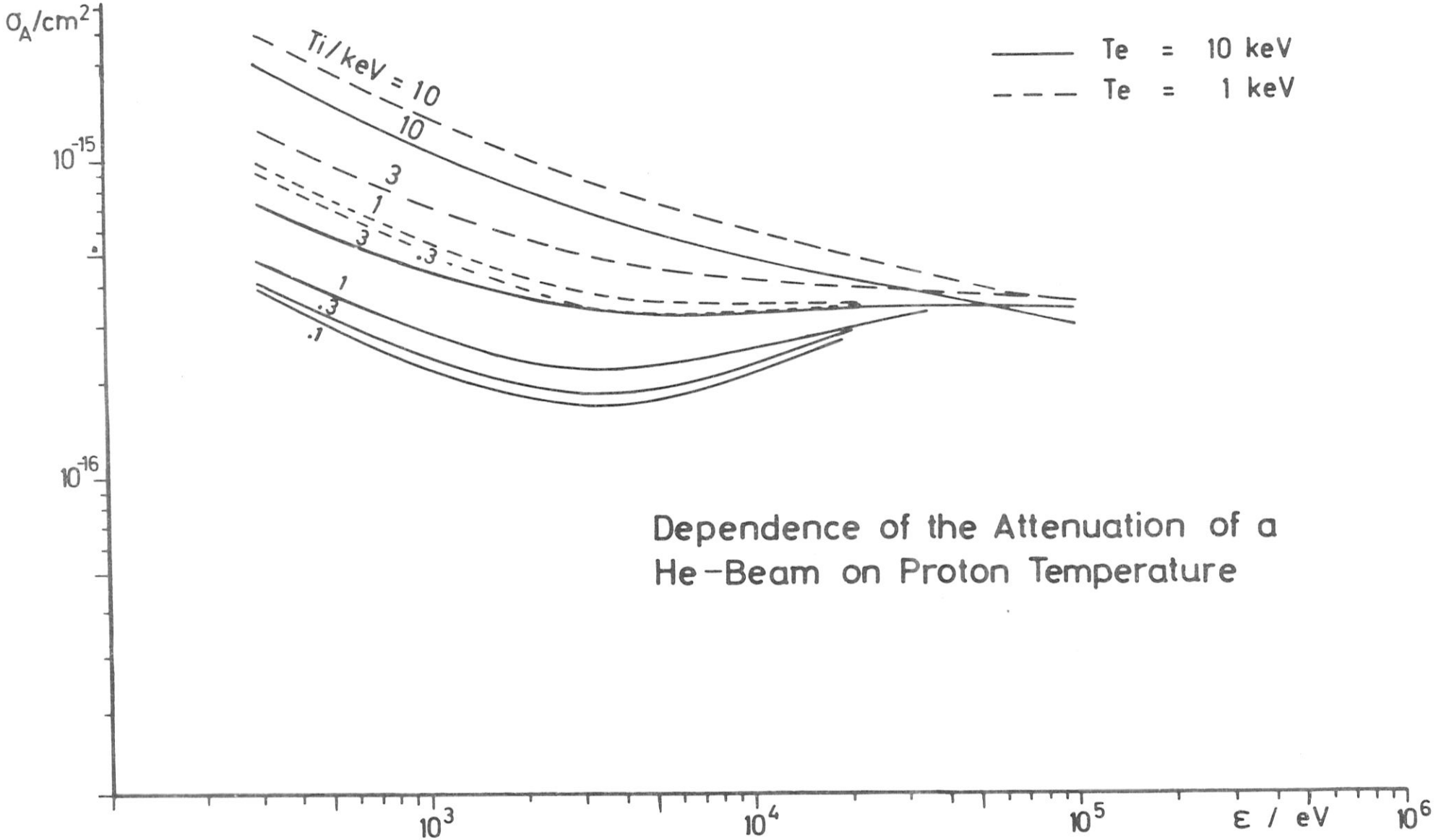

Fig. 3 Variation of the attenuation of a He beam with beam energy for various proton temperatures

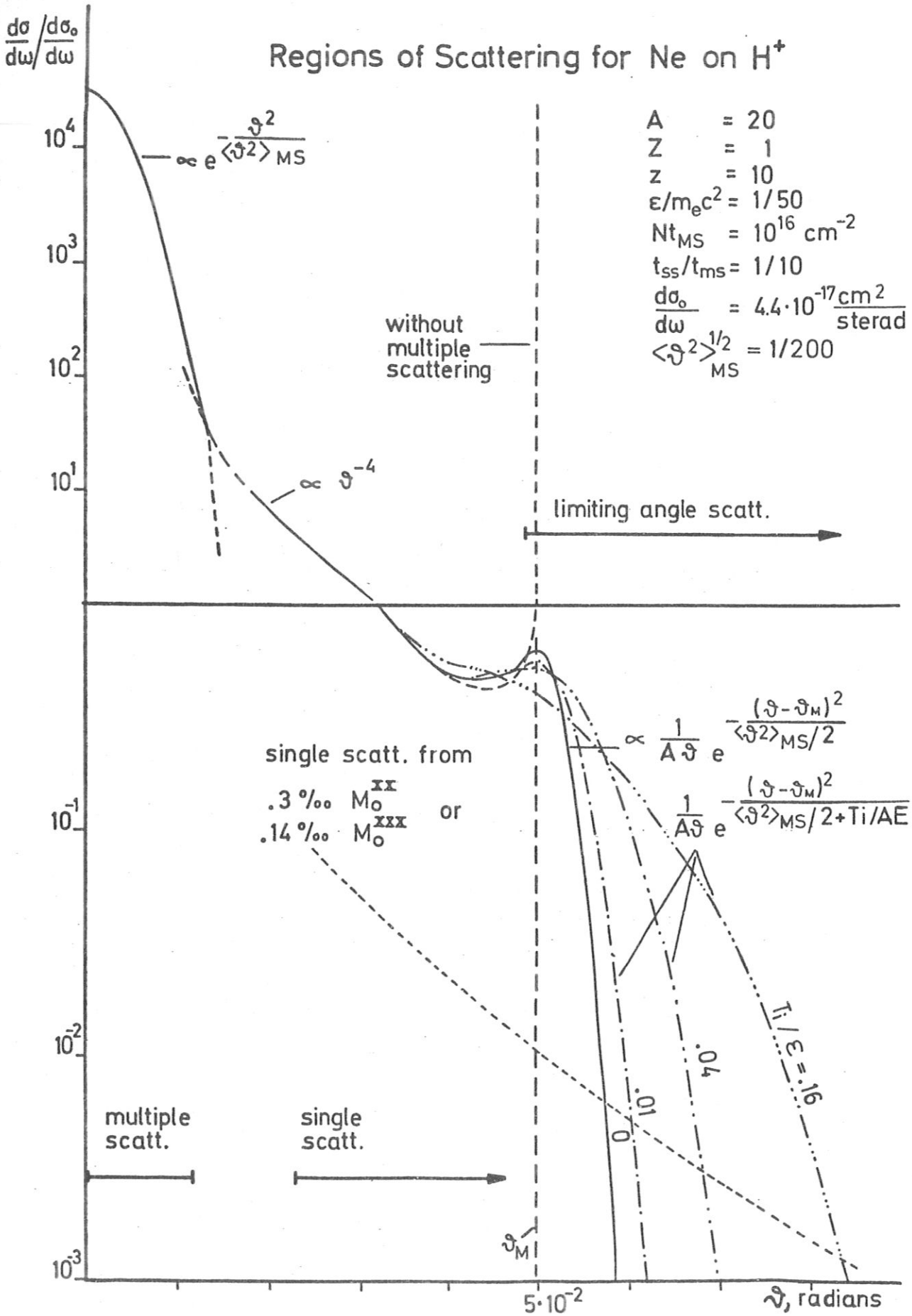

Fig. 4 Scattering profile of a 200 keV Ne-beam